PROPECTS FOR THE USE OF PERMANENT MAGNETS IN FUTURE ACCELERATOR FACILITIES

J. Chavanne, G. Le Bec, ESRF, Grenoble, France

Abstract

Permanent magnet based accelerator magnets may offer a viable alternative to their conventional electromagnetic counterparts for many applications, especially where strong gradients and low power consumption are needed. For example, the development of future light sources based on ultimate storage rings needs to be done in an important energy saving context aiming at a significant reduction in operational costs. After more than two decades of continuous developments in the field of permanent insertion devices, a wealth of knowledge of different issues such as aging effects has been gained. With this technology we now seem ready to leap into the design and construction of advanced accelerator magnets. This talk reviews the status of the permanent magnet technology and the perspectives for its implementations in standard lattice magnets, highlighting both the advantages and the challenges as compared to electromagnetic magnets.

INTRODUCTION

Permanent Magnet (PM) devices of different types have been used in accelerators for more than 20 years; a large majority of them being Insertion Devices (IDs). This is easily explained by a high demand resulting from the construction of many 3rd Generation Light Sources (3GLS) and, more recently, LINAC based Free Electron Lasers (FELs). During these years, the progress made in IDs was significant, the aim being to increase the X-ray brilliance of undulator sources. Issues regarding the PM stability in accelerators has been the object of much attention through many studies on radiation induced demagnetization on the PM arrays of IDs.

Another area of practical interest in PM structures is found in PM multipoles used in the final focus lens in colliders. Here the compactness and performance of the PM structures are important criteria.

To date, there are almost no PM structures used as standard components in accelerator lattices, the lone exception being the Fermilab recycler [1]: a 3.3 km circumference ring based entirely on magnets energized with Strontium ferrites. The choice of ferrite magnet material was motivated by the low field requirements, the low costs and proven stability of the material.

PERMANENT MAGNET MATERIALS

Properties of PM Materials

PM materials combine at room temperature a spontaneous magnetization and coercivity. The spontaneous magnetization is a property of 3d transition metals such as iron, cobalt or nickel. The coercivity is linked to the anisotropy of the material. In modern materials such as Samarium-Cobalt (SmCo) or Neodynium-Iron-Boron (NdFeB), a strong uniaxial magnetocrystalline anisotropy is provided by the rare earth elements Sm or Nd. These compound are usually oriented, using for example the powder metallurgy, to obtain optimal field performance. PM materials are therefore characterized by an easy axis along which usual quantities like the remanence B_r, intrinsic coercivity Hc_j or coercive force Hc_B are given in the manufacturer's data sheets (Figure 1). The general relation between the magnetic induction $\vec{B}$, the magnetization $\vec{M}$ and magnetic field $\vec{H}$ is :

$$\vec{B}(\vec{H}) = \mu_0\left(\vec{H} + \vec{M}(\vec{H})\right) \quad (1)$$

The field performance of a PM device relies primarily on the remanence B_r of the PM material in use. The magnetic stability is a feature of the intrinsic coercivity Hc_J.

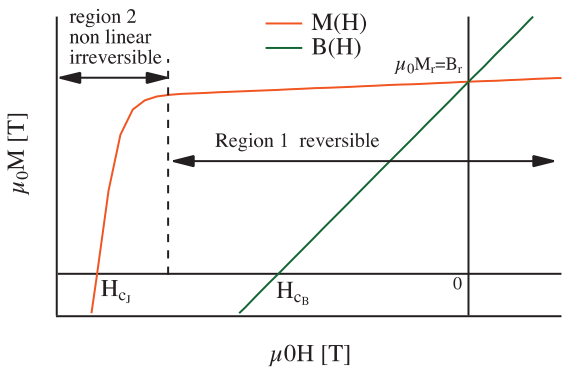

Figure 1: Magnetization curve of a modern PM material and definition of usual magnetic quantities.

For accelerator applications only PM materials with rectangular hysteresis cycles are in use, i.e. materials with $|\mu_0 Hc_J| \geq B_r$. Only materials such as ferrite, NdFeB or SmCo ($SmCo_5$ and Sm_2Co_{17}) can be used therefore. Table 1 gives the typical values for the remanence and coercivity at room temperature of these PM materials. Note that for the NdFeB material, there is a trade off between remanence and coercivity. High remanence grades have moderate coercivity and high coercivity grades have moderate remanence. This feature originates from the amount of additive elements such as Dysprosium (Dy) in the material. The substitution of some amount of Nd by Dy in known to improve the coercivity of the magnet but also to reduce the remanence due to the inverse magnetic coupling between Fe and Dy. However, recent development in NdFeB/PrFeB materials such as

the Grain Boundary Diffusion (GBD) method has shown that the coercivity of these materials can be largely increased by increasing the Dy content at the grain boundaries without impacting on the remanence. This method is however limited by the thickness that can be properly diffused, of the order of a few millimetres.

Table 1: Typical Properties of PM Materials Suitable for Accelerator Systems

Material	Br [T]	μ_0 Hc_j [T]
Strontium Ferrite	0.2 to 0.42	0.2 to 0.4
NdFeB	1.42 to 1.15	1.4 to 3.3
SmCo5	0.8 to 0.9	3
Sm2Co17	1.05 to 1.15	> 2

PM materials are often compared using the maximum energy product $(BH)_{max}$ which represents the maximum density of magnetic energy stored in the material. The comparison of different materials on the basis of this parameter can give, for a given magnetic geometry, an estimate of the relative PM volume necessary to generated the field in the area of interest. Figure 2 shows the evolution of the $(BH)_{max}$ for different PM materials over the last century.

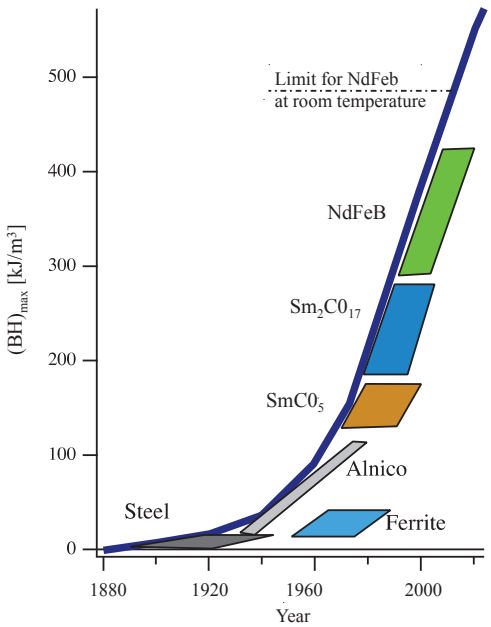

Figure 2: Evolution of the performance of PM materials during the 20th century.

Geometrical Scaling Considerations

From the static Maxwell equations and Equation (1), one can derive the representation of magnetized materials with equivalent fictitious volume and surface current densities $\vec{j}_v$ and $\vec{j}_s$ respectively, both vectors being defined as:

$$\begin{aligned} \vec{j}_v &= \vec{\nabla} \times \vec{M} \\ \vec{j}_s &= \vec{M} \times \vec{n} \end{aligned} \qquad (2)$$

with $\vec{\nabla}$ being the differential operator and $\vec{n}$ the unit vector normal to the boundary of the magnetized media. For magnetic structures built only with magnetized materials such as permanent magnets and iron type pieces, applying a 3D scaling factor k to the structure yields current densities $\vec{j}_v' = \vec{j}_v / k$ and $\vec{j}_s' = \vec{j}_s$ at corresponding points between the initial and scaled structure. From the use of the Biot and Savart law one can easily show that the magnetic field obtained in the scaled structure is the same as in the initial structure. On the other hand, with a similar reasoning using conductors with constant current density, one will obtain a magnetic field reduced by a factor of k in the scaled structure. Obviously, the current density can be adapted to mitigate the scaling effect, however, for scaling factors substantially lower than 1, the current density will, at some stage, be limited by the Joule effect. The only alternative to go beyond this limit is to switch to the superconducting technology. From this brief analysis one can immediately conclude that, for small magnet apertures, PM structures can be extremely compact. Since the present trend in accelerator projects is to reduce the magnet apertures there is consequently an increasing interest for the PM technology. For PM materials with uniform and rigid magnetization, the representation with fictitious current densities reduces to surface densities because the volume component vanishes. The rigidity of the magnetization corresponds to materials with relative permeability equal to 1. This approximation is acceptable for PM material including ferrite, SmCo and NdFeb. In this case magnet blocks can be represented with a Current Sheet Equivalent Model (CSEM) which can be used to evaluate the magnet field of some PM structures with a few per cent error. This method is the basis of the 3D magnetostatic code RADIA developed at the ESRF since 1998 [2].

USE OF PERMANENT MAGNETS IN ACCELERATORS

Synchrotron Light Sources

A common denominator between all 3GLS is the conventional resistive magnet technology used to build up the accelerator lattices and Permanent Magnet (PM) based Insertion Devices (IDs) for the production of high quality X-ray beams [3,4]. PM IDs are also at the heart of LINAC based Free Electron Lasers (FELs) [5,6]. Indeed, high performance NdFeB materials have been used massively for the construction of a large majority of undulators worldwide. The magnetic structures used for IDs are based on Halbach designs [7]. Figure 3 shows schematically the magnetic structures used for undulators, the top part represents a Pure Permanent Magnet (PPM) with 4 blocks /period and the bottom figure shows a Hybrid Permanent Magnet (HPM) structure including

ISBN 978-3-95450-132-8

iron poles. Magnetic periods of undulators are in the range of 10 mm to 400 mm. Because the magnetic field of undulators needs to be varied, the two magnetic arrays are mounted on stiff movable girders placed on either side of a vacuum chamber. The largest field achieved with a PM ID was 3.1 T at a gap of 11 mm and an asymmetric wiggler developed at the ESRF [8].

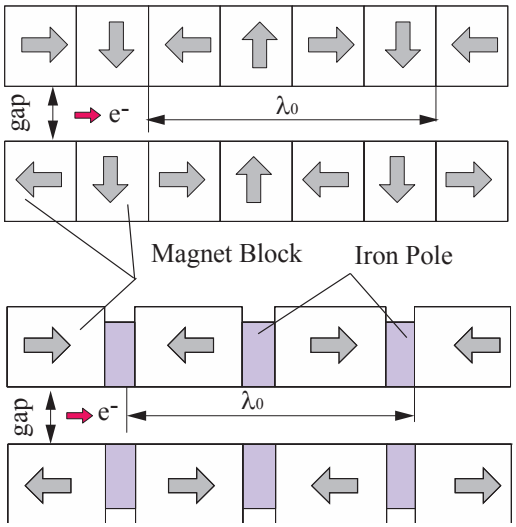

Figure 3: Schematic representation of the two mains magnetic structures used in Insertion Devices.

The peak field B_0 along the electron beam axis can be approximated with a simple expression:

$$B_0 = \alpha B_r \exp(-\beta\pi gap / \lambda_0) \quad (3)$$

where α is a parameter accounting for the magnet technology and β a 3D correction factor (close to 1). Equation (3) suggests that the most obvious way to increase the peak field for a given period is to reduce the minimum gap. However, a limitation is found for conventional IDs due to the required thickness of the vacuum chamber (currently about 10 mm). To remove this limitation, the undulator technology has evolved toward In-Vacuum Undulators (IVUs) with small periods and apertures (Figure 4) [9]. Since 2004, the technology of Cryogenic Permanent Magnet Undulators (CPMUs) has progressively matured as a logical evolution of conventional IVUs [10–12]. With the CPMU technology some limitations found in the performance and stability of permanent magnet materials at room temperature can be overcome. One can highlight the main features of CPMUs as follows:

- Dramatic increase of PM coercivity above 5 T for all NdFeB or PrFeB materials
- Field remanence between 1.55 T and 1.7 T
- Specific $Pr_xNd_{(1-x)}FeB$ are being developed by PM manufacturers [10,13], (Figure 5).

Thanks to the progresses made in the ID technology, the brilliance of 3GLS has been improved by more than one order of magnitude over the last twenty years. However, it clearly appears that the limiting factor for a further significant increase in brilliance is the horizontal emittance of the electron beam which is presently in the range of 1 nm.rad to 4 nm rad. Consequently, the existing magnet lattices of 3GLS need to be replaced by innovative magnet layouts.

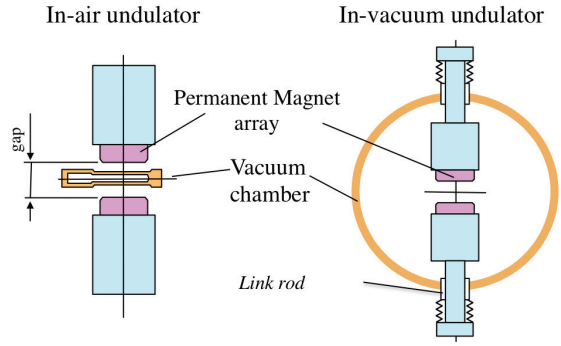

Figure 4: Conventional and in-vacuum undulators.

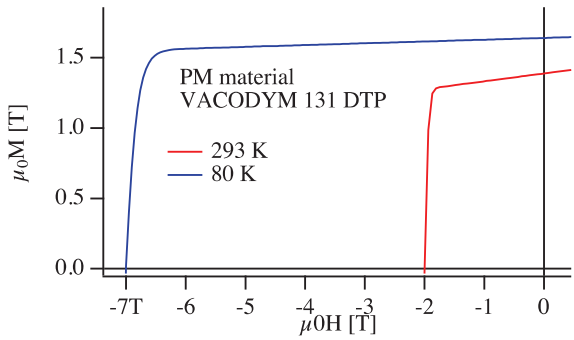

Figure 5: Magnetization curves for a PrFeB type material at room temperature (red) and 80 K (blue).

Recently, a new magnet lattice based on a 7-Bent Achromat (7BA) as adopted for the MAX-IV project [14] was proposed for the 6 GeV storage ring of the ESRF [15]. This concept is being adapted by other facilities such as APS and SPRING8 for similar upgrades. With this new lattice, the ESRF is expecting to reach an electron beam horizontal emittance of about 150 pm which represents a reduction factor of 27 as compared with the existing situation. Because the new lattice must fit in the existing tunnel, a very compact magnet layout is needed. It includes several new types of small aperture magnets such as high gradient quadrupoles with up to 90T/m or moderate field dipole magnets with either longitudinal gradient or transverse gradient. Overall this upgrade project involves the construction of more than 1000 magnets. The energy efficiency of the accelerator complex is one of the constraints defined in the upgrade road map. In light of these considerations, permanent magnet structures are envisioned for some of the lattice components. As a general rule, the PM structures should be as simple as possible with limited field variation in order to be economically viable. The PM structures should combine PM blocks and soft iron (Hybrid devices) to limit the constraints on the magnetic tolerances for the PM blocks. Because of their fixed field, dipoles magnets can be good candidates for a migration to the PMs. The

new lattice of the ESRF storage ring will include 128 dipoles with longitudinal gradient (DLs), each of them being built out of segmented assemblies of 5 dipole modules with different field strengths. Each DL has a length of about 2 m. Figure 6 shows the design of the magnetic field profile of a DL and Figure 7 compares the overall geometry of resistive and PM versions of DLs; both devices have the same aperture of 26 mm at the beam. The weight of the PM versions is three times smaller than that of the resistive version. The PM structure mixes Sm_2C0_{17} and Strontium ferrites in the different modules.

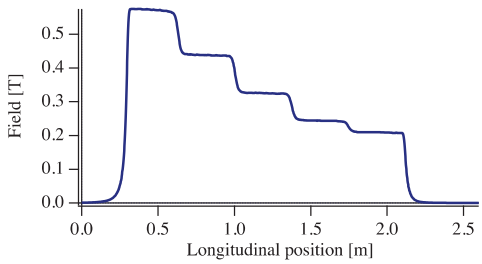

Figure 6: Longitudinal field profile for a DL magnet.

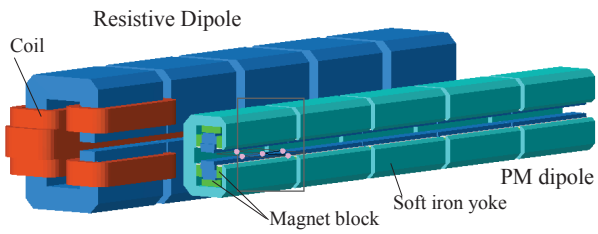

Figure 7: Resistive and PM versions for DL magnets.

PM dipoles are being considered in the SIRIUS project [16] and SPRING8 upgrade project [17].

Colliders

Since the end of the 90s, PM quadrupoles have been developed as components of final focus lenses for colliders [18–20]. The main driving criteria is the compactness of the magnets, the high gradient achievable and low sensitivity to the solenoidal field from adjacent detectors. The 2D theory of multipolar PM structures was initiated by K.Halbach in 1979 on the basis of the CSEM method [21]. For a PM multipole delimited by an inner radius R_1 and an outer radius R_2, the magnetic induction $B(z) = B_y(z) + iB_x(z)$ at position $z = x + iy$ in the magnet aperture is expressed as:

$$B(z) = B_r \frac{n}{n-1}\left(\frac{z}{R_1}\right)^{n-1}\left(1-\left(\frac{R_1}{R_2}\right)^{n-1}\right) \qquad (4)$$

$$\frac{n}{n-1}\left(1-\left(\frac{R_1}{R_2}\right)^{n-1}\right)_{n=1} = \ln(R_2/R_1)$$

where B_r is the remanence of the permanent magnet material. The integer n is the multipole order, n=1 for a dipole, n=2 for a quadrupole … etc. The magnetization inside the PM materials is assumed to vary continuously with the azimuthal angle according to:

$$M(\theta) = M_y + iM_x = M_0 Exp((n+1)i\theta) \qquad (5)$$

Practically, a continuous variation of the magnetization is not feasible. A segmentation approach can be adopted. For a segmented PM structure a more detailed study can be done [21]. The PM multipole can also be built using permanent magnets and iron type material for the poles (hybrid multipole). Figure 8 compares schematically the two types of structures for a quadrupole. The hybrid design is generally more suitable if high field quality is required. Moreover, it can be modified to accommodate coils to add some field variation.

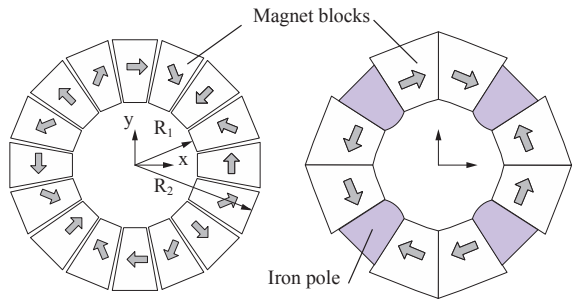

Figure 8: schematic representation of segmented permanent magnet multipole (quadrupole).

Projects of linear colliders such as CLIC are pushing the development of new types of hybrid quadrupoles [22]. Moreover, the project involves also a large quantity of variable field hybrid quadrupoles [23]. In many cases variable field multipoles are based on the mechanical adjustments of PM structures. For systems with tight requirements for the transverse stability of the magnetic axis the movable option may require challenging and costly engineering [24, 25].

MAGNETIC STABILTY OF PM STRUCTURES

Time Stability

A magnetized permanent magnet is in a metastable energy state which is separated from a lower energy state by energy barriers linked to the coercivity of the material. The lower energy state corresponds to a reduced magnetization reached through thermal activation. It corresponds to a statistical process which has been studied by several authors [26, 27].

At a constant temperature the magnetization changes linearly with the logarithm of time:

$$\Delta M = M(t,H) - M(t_0,H) = -s(H)\ln\frac{t}{t_0} \qquad (6)$$

where s is the so called magnetic viscosity and t and t_0 are the times elapsed from the initial magnetization of the material. This representation is generally valid for a limited time interval. However, several experiments show that it is still appropriated for typically periods of several years [28]. The magnetic viscosity depends on the field H. It increases when the field in the magnet material

ISBN 978-3-95450-132-8

approaches the intrinsic coercive field Hc_j where it reaches a maximum. Since the magnetic field of a PM structure depends linearly on the magnetization of the permanent magnets, the relative change on magnetic induction in the magnet aperture will follow that of the magnetization:

$$\frac{\Delta B}{B_0} = \frac{\Delta M}{M_0} = -\frac{s}{M_0}\ln(t/t_0) = -\lambda \ln(t/t_0) \qquad (7)$$

where B_0 and M_0 are the induction and magnetization at time t_0 respectively. The stability of Strontium ferrite was investigated for the construction of the Fermilab recycler [29]. Typical values of λ=1 10^{-4} were measured corresponding to a relative field degradation lower than 10^{-3} between 10 days and 30 years after the initial magnetization of the magnet blocks. Similar studies on NdFeB/Sm_2Co_{17} type magnets have been done mostly to investigate the stability of these materials at high temperature but without enough accuracy to measure small changes at room temperature [28,30]. However, these materials have, at room temperature, a lager ratio $\mu_0 Hc_j/Br$ which suggests a smaller magnetic viscosity than with ferrite type magnets. Nevertheless, dedicated measurements on relevant magnet prototypes should be done. The time stability can be improved using a pre-thermal treatment of the permanent magnet material. The operation consists of temporarily moving the working point (H,M) in the magnet closer to the intrinsic coercivity Hc_j. With this method, the magnet material experiences a small loss in magnetization (generally smaller than 1%) which "removes" the residual weaknesses of the permanent magnets after manufacture. This process is commonly done for PM blocks used in accelerator magnets since it also stabilises the materials against radiation induced demagnetization [31].

Temperature Compensation

PM materials properties are temperature sensitive. Table 2 shows the temperature coefficients of the remanence and intrinsic coercivity for different PM materials. The field of a PM structure will change with temperature according to the temperature dependence of the remanence.

Table 2: Temperature Coefficients of Remanence and Coercivity for Different Types of PM Materials

Material	αBr [%/C]	αHc_j [%/C]]
Strontium Ferrite	-0.2	0.27
NdFeB	-0.08 ,-0.11	-0.5, -07
$SmCo_5$	-0.04	-0.2
Sm_2Co_{17}	-0.03	-0.18

For PM devices with integrated field tunability by means of mechanical or electrical tuning, the impact of temperature variations can be easily compensated. For structures without any active correction, a passive method based on commercially available Fe-Ni alloys [32] having a curie temperature at 40-100 deg C can be used [33]. As such, the magnetization of this material decreases strongly as the temperature increases. These materials have a typical temperature coefficient of -2.5 %/C which is considerably higher than the temperature coefficients of Br for PM materials. It is used to shunt some magnetic flux away from the region of interest, the amount of shunted flux being strongly dependent on temperature. This method of temperature compensation is used for the design of the PM DLs at the ESRF.

Radiation Damages

Radiation induced demagnetization has been a recurrent subject in 3GLS since the early 90s due to the development of small gap IDs. Generally, the field loss in undulators due to radiation induced demagnetization varies along the undulator. In some cases, it can be partially compensated with a small longitudinal gap tapering. For an undulator, a field loss of 0.2 % can impact significantly on the quality of the X-ray spectrum. This has triggered several studies on the radiation hardness on different PM materials [34–40]. The main outcomes from these studies are the following:

At room temperature, the Sm_2Co_{17} material shows the highest radiation hardness with respect to all types of radiation. NdFeB can have comparable resistance if the material has sufficiently high coercivity ($\mu_0 Hc_j$> 3T) and includes a pre-heat treatment.

The resistance to radiation induced demagnetization of NdFeB/PrFeB materials is dramatically increased by cooling at cryogenic temperature. The cooled materials reach a similar level of resistance as that of Sm_2Co_{17} at room temperature.

The demagnetization mechanisms are similar to that resulting from a heating of the magnets. The full magnetization can be restored by a re-magnetization of the material. It suggests a process induced by thermal local spikes occurring at the grain boundaries of the NdFeB materials. Indeed, the coercivity of NdFeB material is mainly dominated by the nucleation of domains with reversed magnetization at the grain boundaries where the anisotropy is reduced. The best candidates for initiating thermal spikes are photo-neutrons generated in the showers behind the incident electrons in the material. Overall, and depending on the selected PM material, the field of a PM structure can experience a slow degradation versus time under radiation exposure. The fundamental question is therefore to determine the lifetime of a PM structure while preserving the required performance [40].

CONCLUSION

PM structures have been advantageously used in several areas of accelerators. The choice is generally dictated by compactness and performance. Future accelerators seem to favour a more intensive use of PM materials due to the reduction of magnet apertures and the

need to reduce the running costs of the accelerators. Studies related to the stability of PM devices for accelerators have made noticeable progresses during the past years. This area will probably receive additional attention in the near future.

REFERENCES

[1] G.W. Foster, Genoa, June 2008, p. 189, (2008), http://www.JACoW.org

[2] O.Chubar, *et al.*, *Journal of Synchrotron Radiation,* vol. 5, pp. 481-484, 1998.

[3] J.Chavanne, P.Elleaume, EPAC 2006, Edinburgh, June 2006, p. 969 (2006); http://www.JACoW.org

[4] M.E. Couprie, IPAC2013, Shanghai, May 2013, p. 26 (2013), http://www.JACoW.org

[5] J.Plueger et al., FEL2013, New York, August2013,p. 367, (2013), http://www.JACoW.org

[6] R. Ganter et al., FEL2012, Nara, August2012, p. 583, (2012), http://www.JACoW.org

[7] K. Halbach., *Nucl. Instr. Meth A,* vol. 187, pp. 109-117, (1981).

[8] J.Chavanne, *et al.*, *Nucl. Instr. Meth A ,* vol. 421, pp. 352-360, (1999).

[9] T. Tanaka et al, FEL2005, August 2005, p. 370, (205), http://www.JACoW.org

[10] Toru Hara et al., Phys. Rev. ST Accel. Beams 7, 050702 (2004).

[11] J. Chavanne et al., PAC09, Vancouver, May 2009, p. 2415 (2009), http://www.JACoW.org

[12] C. Benabderrahmane et al., Nucl. Instr. Met. A 669, (2012).

[13] F. Boergermann et al., TUPRO085, IPAC'14, to be published.

[14] M. Eriksson et al., IPAC2011, San Sebastian, September 2011, p. 3026 (2011), http://www.JACoW.org

[15] L. Farvacque et al., " IPAC2013, Shanghai, May 2013, p. 79 (2013), http://www.JACoW.org

[16] L. Liu et al., "Update on Sirius, The New Brazilian Synchrotron Light Source", MOPRO048, IPAC'14, to be published.

[17] T. Watanabe et al., TUPRO092, IPAC'14, to be published.

[18] Y. Iwashita et al., PAC03, Portand, May 2003, p. 2198 (2003), http://www.JACoW.org

[19] J.K. Lim et al., Phys. Rev. ST Accel. Beams 8, 072401 (2005).

[20] S. Tomanssini et al., PAC07, Albuquerque, June 2007, p. 1466, (2007), http://www.JACoW.org

[21] K. Halbach,, Nucl. Instr. Meth. 169, p. 1, (1980).

[22] M. Modena et al,, IPAC1012, New Orleans, May 2012, p. 3515, (2012), http://www.JACoW.org

[23] B.J.A Shepherd et al, Shanghai, May 2013, p. 3606, (2013), http://www.JACoW.org

[24] Volk J.T. et al., PAC2001. May 2001, Chicago, (2001), http://www.JACoW.org

[25] Shepherd B. et al, CLIC workshop, CERN, February 2014.

[26] Néel, Louis, J. de Phys. et Radium, 11, 461, (1950).

[27] Street R. and Wooley. J.C., Proc. Phys. Soc. A62, 562-572, (1949).

[28] M. Haavisto al, IEEE trans. Mag., Vol. 45, (12), p.5277, (2009).

[29] H.D. Glass al, PAC97, May 1997, p. 1260, (1997), http://www.JACoW.org

[30] Liu J. al, Proc. Space Nuclear Conf., Boston, June 2007.

[31] T. Bizen et al., Nucl. Instr. Meth. 515 (2003) 850–852.

[32] See for example "Soft magnetic materials and semi-finished products", Vacuumschmelze brochure Pb-pht-1.pdf.

[33] Bertsche K. et al., PAC95. May 1995, Dallas, (1995), http://www.JACoW.org

[34] T. Bizen et al., Nucl. Instr. Meth. A, 467-468, pp. 185-189, (2001).

[35] M. Petra et al., Nucl. Instr. Meth. A, 507, pp. 422-425, (2003).

[36] J. Alderman et al., Nucl. Instr. Meth. A, 481, pp. 9-28, (2001).

[37] T. Bizen et al., Nucl. Instr. Meth. A, 574, pp. 401-406, (2007).

[38] T. Bizen et al., EPAC2004, June 2004, Lucerne, p. 2092, (204), http://www.JACoW.org

[39] H.B. Luna et al., Nucl. Instr. Meth. A, 285, pp. 349-354, (1989).

[40] A. B. Temnykh, Nucl. Instr. Meth. A, 587, pp. 13-19, (2008).

ISBN 978-3-95450-132-8